Estimating Workers' Physical Effort during Isometric Contractions through sEMG: The Role of Feature Selection

ROBERTO BILLARDELLO, Università Campus Bio-Medico di Roma, Rome, Italy
CHRISTIAN TAMANTINI, Institute of Cognitive Sciences and Technologies, National Research Council, Roma, Italy
FRANCESCA CORDELLA and FRANCESCO SCOTTO DI LUZIO, Università Campus Bio-Medico di Roma, Rome, Italy
TIWANA VARRECCHIA, GIORGIA CHINI, FRANCESCO DRAICCHIO, and ALBERTO RANAVOLO, Department of Occupational and Environmental Medicine, Epidemiology and Hygiene, INAIL, Monte Porzio Catone, Italy
LOREDANA ZOLLO, Università Campus Bio-Medico di Roma, Rome, Italy

Work-related musculoskeletal disorders represent one main contributor to production workers absenteeism. In industry 5.0, exoskeletons have been proposed to mitigate risks of injury by supporting workers during repetitive tasks, with surface Electromyography (sEMG) showcasing their effects. Although existing studies have primarily evaluated exoskeletons by comparing muscle activity with and without the device, a systematic investigation of which sEMG features most effectively reflect muscle fatigue during prolonged arm elevation is still missing.

This study aims to evaluate the effectiveness of different sEMG features in estimating perceived physical effort during an overhead bolting-unbolting task, performed by 10 participants both with and without a passive shoulder exoskeleton. It further assesses how the use of the exoskeleton influences the fatigue-related

This work was supported partly by the Italian Ministry of Research, under the complementary actions to the NRRP "Fit4MedRob - Fit for Medical Robotics" Grant (#PNC0000007), (CUP: B53C22006990001), the Italian Ministry of Education, Universities and Research (MIUR) with the FAIR project (CUP: C53C22000800006), the European Union's Horizon 2020 research and innovation programme under grant agreement No. 899822 (CUP: C82F20000090006) (SOMA project), and the Italian Institute for Labour Accidents (INAIL) with the SPINE 4.0 project (CUP: C85F21001020001). The research presented in this article was carried out as part of the SOPHIA project, which has received funding from the European Union's Horizon 2020 research and innovation program under Grant Agreement No. 871237 and partially funded by the European Union—NextGenerationEU under the cascade call for proposals for research activities "Age-It—Ageing Well in an Ageing Society, OPERA subproject" (PNRR Mission 4, Component 2, Investment 1.3, CUP: B83C22004800006).
Authors' Contact Information: Roberto Billardello (corresponding author), Università Campus Bio-Medico di Roma, Rome, Italy; e-mail: roberto.billardello@gmail.com; Christian Tamantini, Institute of Cognitive Sciences and Technologies, National Research Council, Roma, Italy; e-mail: christian.tamantini@cnr.it; Francesca Cordella, Università Campus Bio-Medico di Roma, Rome, Italy; e-mail: f.cordella@unicampus.it; Francesco Scotto di Luzio, Università Campus Bio-Medico di Roma, Rome, Italy; e-mail: f.scottodiluzio@unicampus.it; Tiwana Varrecchia, Department of Occupational and Environmental Medicine, Epidemiology and Hygiene, INAIL, Monte Porzio Catone, Italy; e-mail: t.varrecchia@inail.it; Giorgia Chini, Department of Occupational and Environmental Medicine, Epidemiology and Hygiene, INAIL, Monte Porzio Catone, Italy; e-mail: g.chini@inail.it; Francesco Draicchio, Department of Occupational and Environmental Medicine, Epidemiology and Hygiene, INAIL, Monte Porzio Catone, Italy; e-mail: fdraicc@gmail.com; Alberto Ranavolo, Department of Occupational and Environmental Medicine, Epidemiology and Hygiene, INAIL, Monte Porzio Catone, Italy; e-mail: a.ranavolo@inail.it; Loredana Zollo, Università Campus Bio-Medico di Roma, Rome, Italy; e-mail: l.zollo@unicampus.it.

ACM 2573-9522/2025/9-ART15
https://doi.org/10.1145/3759159

metrics identified. sEMG signals were collected from seven bilateral muscle groups, and 15 time-, frequency-, and spatial-domain features were extracted and correlated with two subjective effort perception models.

Our results highlight strong correlations between time-domain features and perceived physical effort. Moreover, comparisons between conditions demonstrate that the exoskeleton provides a measurable fatigue-reducing effect. In contrast, spatial-domain features showed weak associations with perceived effort, suggesting limited suitability for low-intensity, long-duration tasks. These findings contribute to identifying the most informative sEMG features for fatigue estimation and provide evidence of the benefits of passive exoskeletons in industrial scenarios.

CCS Concepts: • **Computing methodologies** → Feature selection; • **Hardware** → *Biology-related information processing*; • **Human-centered computing** → *Empirical studies in interaction design*;

Additional Key Words and Phrases: sEMG, Exoskeleton, Ergonomics

ACM Reference format:
Roberto Billardello, Christian Tamantini, Francesca Cordella, Francesco Scotto di Luzio, Tiwana Varrecchia, Giorgia Chini, Francesco Draicchio, Alberto Ranavolo, and Loredana Zollo. 2025. Estimating Workers' Physical Effort during Isometric Contractions through sEMG: The Role of Feature Selection. *ACM Trans. Hum.-Robot Interact.* 15, 1, Article 15 (September 2025), 21 pages.
https://doi.org/10.1145/3759159

1 Introduction

Musculoskeletal disorders represent a significant health problem, being the most common work-related injury in the European Union and one of the primary causes of work absenteeism [1, 2]. In 2019, these disorders were estimated to affect approximately 150 million Europeans [3, 4]. A large number of studies highlighted the contribution of common work activities to the development of **work-related musculoskeletal disorders (WMSDs)**, such as repetitive and prolonged tasks, improper postures, and fatigue [5–8]. In Industry 4.0, and more recently with the human-centric approach of Industry 5.0, wearable devices [9–11], the reorganization and instrumentation of workstations [12, 13], and the use of industrial exoskeletons have been proposed to reduce the risk of WMSDs by supporting workers in prolonged or repetitive tasks [14–17]. The growing interest in exoskeletons stems from their ability to provide various types of assistance to the human joints, thereby reducing the muscular effort while maintaining their freedom of movement as naturally as possible [16, 18]. Exoskeletons can be classified by the body district they support or by their actuators: active systems use powered actuators while passive systems rely on mechanical structures. Semi-passive systems can provide selective assistance during specific movement phases by integrating both active and passive elements [19]. Independently of the presence of actuators, exoskeletons supporting the shoulder joint are highly valuable in industrial environments, where overhead work represents a well-established risk factor for WMSDs [16, 18, 20, 21].

However, there is a growing need to test and validate these devices to assess their ability to reduce workers' physical workload, which is closely linked to the risk of developing WMSDs. In this domain, **surface electromyography (sEMG)** has emerged as a prevalent technique [14, 22, 23] for evaluating exoskeleton effectiveness in reducing muscle effort and detecting potential adverse effects, such as altered muscle activation [18] or increased discomfort in non-targeted areas [1, 24]. Moreover, while temporal- and frequency-domain features correlate with physical workload, recent **high-density sEMG (HDsEMG)** studies showed that spatiotemporal sEMG distribution also changes significantly with muscle fatigue or pain [25–28]. An additional benefit of HDsEMG over bipolar sEMG is its denser spatial distribution, enabling motor unit activity extraction through decomposition algorithms [29, 30], and the identification of different activation

foci [31–33]. Moreover, studies showed that pain can significantly alter muscle activation patterns and increase fatigue [26, 34]. Since prolonged physical workload and muscle fatigue are well-established contributors to injury risk, sEMG-based analysis offers a valuable indirect means of informing risk assessment strategies. However, despite their recognized potential to capture signs of fatigue or pain, and thus increased injury risk, the use of spatial features derived from HDsEMG for accurate fatigue estimation in occupational settings holds significant promise but remains largely unexplored [35]. The absence of comprehensive analyses conducted in real-life occupational environments hinders the translation of these promising markers into practical tools for the early identification and prevention of WMSDs.

In addition to muscle activation assessments, only a few studies have monitored cardio-respiratory activities, using physiological parameters like **heart rate (HR)** and **respiration rate (RR)**, during tasks [36, 37]. Nonetheless, combining these parameters with perceived effort questionnaires can help gauge physical workload and validate the effects of devices, as changes in HR and RR have been, in fact, associated with fatigue and intense effort [38, 39] and thus can be used to detect the presence of fatigue from an objective point of view [40]. Moreover, although various active [41, 42], passive [18, 43], and semi-passive [44] exoskeletons significantly reduced musculoskeletal loading, studies on changes in sEMG spatiotemporal distribution in real-life occupational settings are limited.

Numerous studies have analyzed body kinematics to detect compensatory movements and strategies induced by fatigue [45, 46]. However, when dealing with isometric contractions, sEMG-based approaches may provide more insightful information. Although several studies have investigated various sEMG-derived measures to identify muscular fatigue, only a few have comprehensively compared features across different signal domains [35, 47–50]. Numerous studies have achieved high accuracy in distinguishing fatigued from non-fatigued states using traditional machine learning and deep learning classifiers [50–54]. However, these studies typically use a binary approach, which neglects the continuous progression of muscular fatigue. In this context, Frey-Law et al. [55] proposed and validated a three-compartment muscle fatigue model consisting of active, fatigued, and resting muscle states. The model has been shown to effectively estimate fatigue at the joint level by accurately predicting endurance times during sustained isometric tasks, providing a valuable foundation for modeling localized fatigue in ergonomic and biomechanical applications. However, to effectively monitor and mitigate risks for workers, it is crucial to identify global physical workload levels continuously over time. To achieve this, it is essential to identify metrics that accurately and promptly reflect physical workload trends, enabling the development of intelligent and optimized monitoring systems.

An early attempt at estimating a continuous level of fatigue was made by Yochum et al. [56], who proposed a functional electrical stimulation system capable of also indicating the intensity of muscular fatigue during exercise through sEMG recordings. In their study, muscle fatigue was estimated on a scale from 0% to 100% based on M-wave duration, an electrical activity that follows stimulation pulses. A value of 0% corresponded to a non-fatigued muscle (i.e., at the onset of stimulation), while a value approaching 100% indicated substantial muscular fatigue, characterized by a doubling of the M-wave duration ($s = 2$). In recent years, to address these limitations and obtain a continuous measure of muscle effort, Divekar et al. [57] computed muscle effort as the mean **root mean square (RMS)** of the EMG signal, normalized to the percentage of maximum voluntary contraction (%MVC) over the gait cycle. In related studies, Kuber et al. [58, 59] evaluated perceived effort using the Borg scale, while Bergmann et al. [60] developed a mathematical model based on user-generated force/torque inputs, while still reporting subjective fatigue over time. However, these approaches are susceptible to individual variability, such as participant motivation, and are typically task-specific, focusing on particular muscles and thereby limiting their generalizability

for estimating overall fatigue levels. To address these limitations, Jin et al. [61] incorporated physiological signals, including HR and functional near-infrared spectroscopy, to classify 16 distinct workload levels. Similarly, Forman et al. [62] associated perceived effort with frequency-domain features of physiological signals. In their work, Coraggio et al. [63] compared multiple fatigue-related metrics against exercise repetition counts to identify the most fatigue-sensitive indicators. However, their analysis was restricted to the lateral deltoid and middle trapezius muscles and did not account for the influence of assistive devices such as exoskeletons, which may attenuate fatigue development. The increasing interest in these solutions and the limited systematic comparison of sEMG features across time, frequency, and spatial domains highlight the need for more targeted analyses. Such comparisons can enhance our understanding of how different features correlate with physical workload models and their evolution over time, thereby improving the effectiveness of ergonomic interventions.

The primary objective of this study is to evaluate the effectiveness of surface EMG features from different domains (time, frequency, and spatial) in estimating perceived physical effort and detecting muscle fatigue during a prolonged low-intensity overhead task. A secondary objective is to assess how the use of a passive shoulder exoskeleton influences the evolution of fatigue-related metrics over time. To this end, we designed an experimental protocol simulating an industrial scenario in which 10 participants performed a repetitive overhead bolting-unbolting task under two conditions: **with (W)** and **without (WO)** a passive shoulder exoskeleton. As the task required both arms to perform the same repetitive action simultaneously on two separate bolts, we recorded sEMG signals from seven muscle pairs, using bipolar electrodes on the non-dominant side and HDsEMG on the dominant side. This setup enabled a comprehensive assessment of muscle activity, capturing both global effort and spatial activation patterns. In addition to evaluating temporal and frequency features, we analyzed changes in the spatial distribution of muscle activation (from HDsEMG) and monitored cardio-respiratory activity to complement the effort assessment. Lastly, we assessed the ability of the extracted features to reflect instantaneous effort levels, track fatigue progression over time, and distinguish between working conditions.

The article is structured as follows: Section 2 presents the setup, the features extracted in the study, the experimental protocol, and the conducted analysis. Results are illustrated and discussed in Section 3. Section 4 contains a discussion on the work, and finally, Section 5 contains conclusions and some future extensions of the work.

2 Material and Methods

The workflow of the study is shown in Figure 1: bipolar sEMG, HDsEMG, and cardio-respiratory parameters (i.e., HR and RR) were acquired from the subjects performing an overhead task in the W/WO conditions. sEMG signals were pre-processed, and features from the time, frequency, and spatial domains were extracted. Two physical effort models were proposed and correlated to the extracted features: a linear model with a positive slope and an exponential model based on RC circuit capacitor charging [64]. Features were ranked by correlation level, with the most relevant ones analyzed further to assess their ability to distinguish fatigue levels in both conditions. Each step of the workflow will be detailed in the following sections.

2.1 Experimental Setup

Bipolar sEMG and HDsEMG sensors were placed on key muscles commonly monitored in shoulder exoskeleton studies [22]. HDsEMG grids were positioned on the dominant side's **biceps brachii (BI)**, **triceps brachii (TR)**, **latissimus dorsi (LD)**, and **anterior deltoid (AD)**. Bipolar sEMG sensors were placed on both sides' **medial deltoid (MD)**, **upper trapezius (UT)**, and **rectus abdominis (AB)** and on the non-dominant side's BI, TR, LD, and AD for direct comparison with

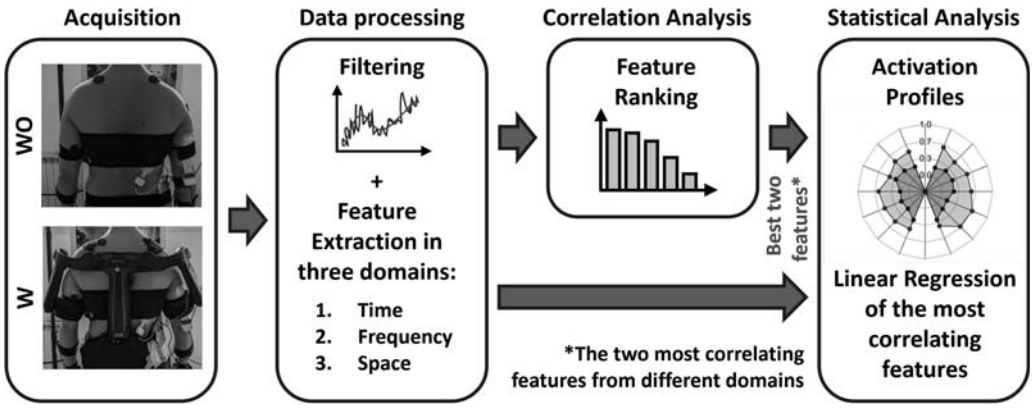

Fig. 1. Workflow of the study—from left to right: execution of the task and data acquisition; data processing and feature extraction; analysis of the correlations between features and fatigue (WO condition); statistical analysis.

HDsEMG. To reduce electrode-skin impedance, subjects' skin was cleaned with alcohol before electrode placement. HDsEMG reference electrodes were positioned on the wrist (for BI and TR) and clavicle (for AD and LD). All EMG sensors were placed following SENIAM guidelines [65].

HDsEMG utilized three Sessantaquattro systems (OT Bioelettronica, Torino, Italy, sampling frequency: 2 kHz) with two 64-channel grids (5×13) for the BI and TR muscles and two 32-channel grids (4×8) for the LD and AD (1-mm diameter, 8-mm inter-electrode distance). Electrodes were attached using double-sided adhesive foam (SPES Medica, Genoa, Italy) and electro-conductive paste (SPES Medica).

Delsys Trigno bipolar sEMG electrodes (Delsys, Massachusetts, USA, sampling frequency: 1.11 kHz, Inter-electrode spacing: 10 mm) were placed on the dominant side MD, UT, and AB and all muscles on the non-dominant side.

HR (electrocardiography sampling frequency: 250 Hz) and RR (breathing waveform sampling frequency: 25 Hz) were measured with the BioHarness 3.0 chest belt (ZephyrTM Technology, Medtronic, Dublin, Ireland).

The MATE-XT exoskeleton (COMAU, Italy) was used in the W condition. This commercial system provides support to the shoulder with an adjustable spring-based torque for gravity compensation [66]. The support level was individually adjusted based on the manufacturer's recommendations, in accordance with the weight and the height of the subjects. All sensors were synchronized with an external trigger using an OT Bioelettronica synch-station. The full setup is shown in Figure 2.

2.2 Subjects and Experimental Protocol

Participants provided written informed consent after receiving a thorough explanation of the experimental procedure and prior to participating in the study, which adhered to the Helsinki Declaration and was approved by the local ethics committee.

Ten healthy male subjects (27 ± 2 years; weight: 81 ± 8 kg; height: 180 ± 7 cm) were involved in the study (local ethics committee approval: N.0078009/2021). Exclusion criteria included inability to give informed written consent, history of musculoskeletal disorders, upper limb, lower limb, or trunk surgery, orthopedic or neurological diseases, disorders of the vestibular system, visual impairments or back pain, current pharmacological treatment, and obesity (defined as a body mass index $\geq 30\,kg/m^2$). Additionally, female participants were excluded to avoid potential variability due to anatomical and physiological differences that could influence the analysis of muscular

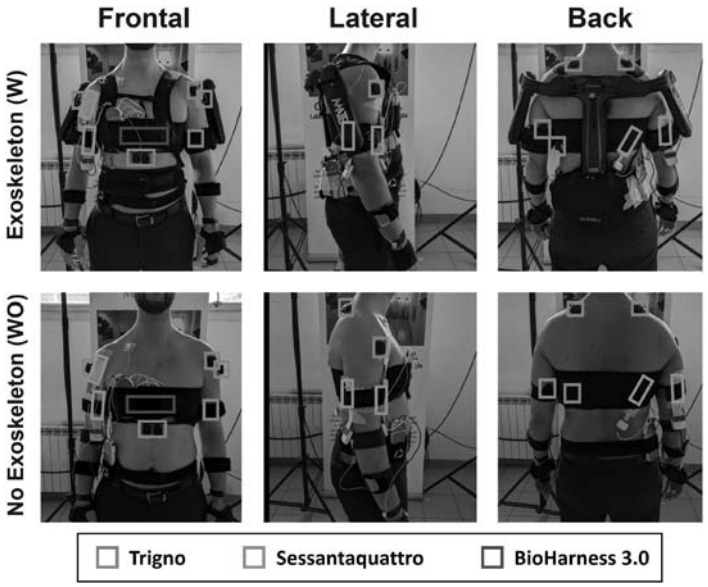

Fig. 2. Experimental setup—a representative participant wearing the MATE-XT passive exoskeleton along with the multimodal monitoring system: Delsys Trigno (green), OT Bioelettronica Sessantaquattro (blue), ZephyrTM BioHarness 3.0 (red).

responses. Only male participants were recruited in order to control for potential variability related to sex-specific differences in muscle morphology and fatigue responses, as previously reported in the literature [67, 68]. Before task execution, a 5-minute baseline was recorded to measure HR and RR while subjects were seated in a resting condition.

The task was selected to induce progressive upper limb fatigue while simulating a real working scenario. Participants performed a bilateral, continuous overhead bolting-unbolting movement, maintaining an isometric contraction by holding the shoulder and elbow joints at 90° of flexion throughout the task (Figure 3). The height of the structure was adjusted for each subject, who was instructed to maintain a consistent bolting-unbolting pace with both hands. The task lasted up to 15 minutes or until exhaustion. The order of conditions (W and WO exoskeleton) was randomized to mitigate carry-over effects, with both conditions recorded on the same day, 3 hours apart.

Perceived effort, as well as exoskeleton usability, was assessed using the Borg 6-20 Scale [69] and **system usability scale (SUS)** [70, 71] questionnaires, respectively, administered at the end of each condition. Before completing the Borg scale, participants were instructed to focus their rating specifically on the effort associated with the isometric contraction (i.e., maintaining the arm position), rather than on the screwing activity.

2.3 Data Processing

Bipolar and HDsEMG data processing are presented in Figure 4.

Data were digitally filtered with a fourth-order Butterworth band-pass filter (20–500 Hz). Ten commonly studied features in the time and frequency domains were calculated for bipolar sEMG [47, 72]. In order to directly compare bipolar and HDsEMG data, the same ten features were calculated also for the HDsEMG by averaging the signals of each grid, thus considering the grid as a single virtual electrode.

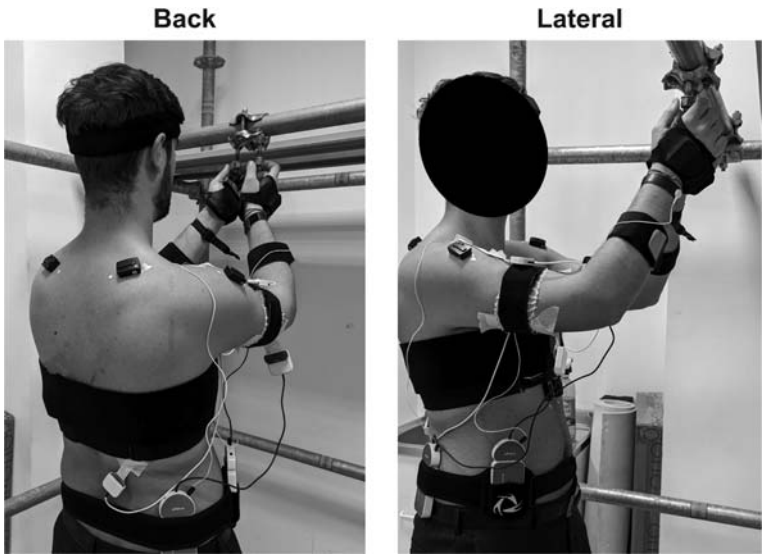

Fig. 3. Overhead bolting-unbolting task. Shoulder and elbow flexed at 90°. The height of the structure is set accordingly to the subject.

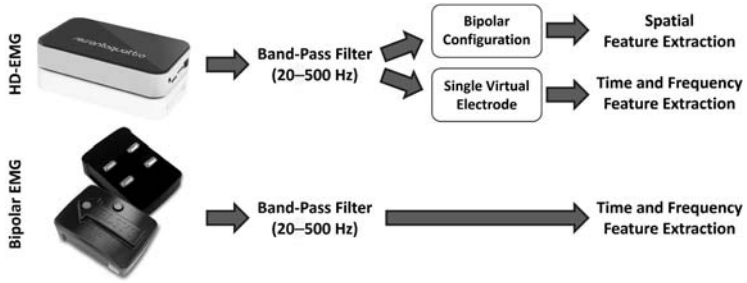

Fig. 4. Bipolar and HDsEMG data processing: from band-pass filtering to feature extraction. Signals from both systems were band-pass filtered between 20 and 500 Hz. HDsEMG signals were further processed to obtain a bipolar configuration for spatial feature extraction, or a single average virtual electrode for time and frequency feature extraction.

Moreover, 59 and 28 bipolar sEMG signals were obtained from each 64- and 32-electrode grids, respectively, by subtracting the signals from two adjacent electrodes along the columns [73]. The obtained bipolar grids were used to extract spatial features [31–33, 72]. All features from bipolar sEMG, HDsEMG, and cardio-respiratory signals were calculated on non-overlapping time windows of 30 seconds. Time- and frequency-domain features were normalized per subject in the 0–1 range, while space-domain features were expressed in the grid coordinate reference system. To study the variation of the features with the increasing of fatigue, the obtained observations were organized in three equally distributed time frames, expressed in minutes: start ($0 \leq time < 5$), middle ($5 \leq time < 10$), and end ($time \geq 10$).

HR and RR were normalized, for each subject, with respect to their baseline value, and their increase percentages were calculated and averaged—for each condition and time frame. Similarly to sEMG data, data were organized in three equally distributed time frames.

2.3.1 Time-Domain Features. Time-domain features describe the signals behavior in the time dimension and represent the most popular approach to study physical workload [72]. Previous studies showed that features in this domain present an increasing trend over time [74, 75]. We computed:

—*RMS*: RMS of a signal is related to the average activation level of the signal, and it can be calculated as

$$\text{RMS} = \sqrt{\frac{1}{N}\sum_{i=1}^{N} x_i^2}, \tag{1}$$

where N is the number of elements in the 30-second time window (N = 33,333 in bipolar sEMG, N = 60,000 in HDsEMG), x_i is the value of the sEMG signal of the ith sample.

—*Simple Square Integral (SSI)*: similarly to RMS, also SSI is related to the average activation of the signal, and it can be calculated as

$$\text{SSI} = \sum_{i=1}^{N} (x_i)^2 . \tag{2}$$

—*Zero Crossing (ZC)*: ZC is calculated as the number of times the sEMG signal changes its sign. This measure is related to muscle contraction and can be expressed as

$$\text{ZC} = \frac{1}{2}\sum_{i=1}^{N-1} |\text{sign}(x_i) - \text{sign}(x_{i+1})|, \tag{3}$$

where sign(x) represents the sign function, which returns -1 if $x < 0$, 0 if $x = 0$, and 1 if $x > 0$

—*Wavelength (WL)*: WL measures the cumulative length of a signal waveform as

$$\text{WL} = \sum_{i=1}^{N-1} |x_{i+1} - x_i|. \tag{4}$$

—*Variance (VAR)*: VAR is a statistical measure that quantifies the dispersion or spread of a set of values around their mean. Mathematically

$$\text{VAR}(x) = \frac{1}{N}\sum_{i=1}^{N}(x_i - \bar{x})^2, \tag{5}$$

where $\bar{x}$ represents the average value of the signal in the time window.

—*Mean Absolute Value (MAV)*: MAV quantifies the average magnitude of a signal over a certain window or set of samples as

$$\text{MAV} = \frac{1}{N}\sum_{i=1}^{N} |x_i| \tag{6}$$

2.3.2 Frequency-Domain Features. Frequency-domain features can be obtained from the calculation of the power spectrum of the signal through methods like the Fourier Transform. Contrary to time-domain features, when muscle fatigue occurs, features from this domain tend to decrease over time [74, 75].

—*Mean and Median Power Frequency (MeanF and MedF)*: MeanF and MedF are commonly used measures in signal processing, particularly in the analysis of power spectra. These features are

characterized by a linear decrease with physical workload over time. Mathematically

$$\text{MeanF} = \frac{\sum_f f \cdot P(f)}{\sum_f P(f)}, \tag{7}$$

where *P(f)* represents the power spectrum of the signal, calculated through Discrete Fourier Transform;

—While MedF*(t)* was obtained by:

(a) Arranging the power spectrum *P(f)* in ascending order.
(b) Calculating the cumulative sum of power values.
(c) Finding the frequency bin where the cumulative sum reached half of the total power.

—*Instantaneous Mean and Median Frequency (IMeanF and IMedF)*: Instantaneous frequency can be determined using the Hilbert Transform, and it allows tracking the evolution of the frequency of a signal dynamically. Similarly to MeanF, IMeanF can be calculated as

$$\text{IMeanF}(t) = \frac{\sum_f f \cdot P(f,t)}{\sum_f P(f,t)}. \tag{8}$$

—While IMedF*(t)* was obtained by:

(a) Calculating the instantaneous frequency power *P(f,t)*.
(b) Calculating the frequency-averaged frequency power *Pf(t)* by averaging *P(f,t)* across the frequency domain for each time point *t*.
(c) Calculating the cumulative sum of values of *Pf(t)*.
(d) Finding the frequency bin where the cumulative sum reached half of the total power.

Both IMeanF and IMedF showed a downward trend with increasing fatigue.

2.3.3 Space-Domain Features. RMS values extracted for each electrode in HDsEMG grids can be used to create topographical maps. The use of these maps allows the identification of adjustments in the muscular activity across specific muscle areas, such as changes in the position of the activation focus or its homogeneity [31–33].

—*Region of Activation (RoA)*: RoA is defined as the position (in electrode coordinates) of the center of the 4-electrodes neighborhood with the highest average RMS [31]. Neighborhoods were made of two rows and two columns of adjacent electrodes. X and Y coordinates of the center were extracted, with the Y axis parallel to the muscle fiber.

—*Center of Gravity (CoG)*: Similarly to RoA, CoG was calculated from the RMS topographical map, as follows [32, 33]

$$\text{X}_{CoG} = \frac{\sum_i \sum_j i \cdot \text{Ev}(i,j)}{\sum_i \sum_j \text{Ev}(i,j)} \tag{9}$$

$$\text{Y}_{CoG} = \frac{\sum_i \sum_j j \cdot \text{Ev}(i,j)}{\sum_i \sum_j \text{Ev}(i,j)}, \tag{10}$$

where X_{CoG} is the x-coordinate of the CoG, Y_{CoG} is the y-coordinate of the CoG, i and j represent the coordinates of the virtual electrode, $\text{Ev}(i,j)$ represent the value of the electrode at i and j coordinates

—*Entropy (Entr)* [32, 33]: Entr of an image or, in our case, of a two-dimensional signal, can quantify the homogeneity in the distribution of pixel intensities within an image. Entr can be

calculated as

$$\text{Entr} = -\sum_{i=1}^{n} P(Ev) \cdot \log_2(P(Ev)), \tag{11}$$

where $P(x_i)$ is the probability of occurrence of pixel intensity Ev in the image, n is the total number of possible pixel intensity levels. In presence of muscle fatigue, the spatial reorganization of the muscle activity can lead to a reduction of homogeneity (lower entropy) [32, 33].

2.4 Correlation Analysis

Considering the physical effort as a non-decreasing function that increases with time, two mathematical functions were evaluated: a linear model with a positive slope (with its value set to 0 at the beginning of the task and reaching 1 by the end) and an exponential model inspired by the charge of a capacitor in an RC circuit [64], expressed as

$$\text{F(t)} = Qmax\left(1 - e^{-t/RC}\right), \tag{12}$$

where $F(t)$ represents the physical effort as a function of time. $F(t)$ value is set to 0 at the beginning of the task (absence of fatigue) and to 0.9 at the end (high level of fatigue). $Qmax$ and RC are set to 1.

In particular, the linear model was selected as it can directly represent the time elapsed from the beginning of the task. Identifying features that exhibit strong correlation with this model would indicate a direct association with time progression. An example of this approach is found in Alty and Georgakis [76], who used linear regression to assess the temporal behavior of selected features during fatigue-inducing tasks. On the other hand, the RC circuit-inspired model originates from the work of Peternel et al. [64], who proposed a robotic assistance framework based on fatigue detection. Unlike the linear model, this approach assumes a more rapid increase in fatigue levels followed by an early saturation, similar to the results based on the perceived effort obtained by Ratke et al. [51]. Correlation coefficients between the features and the two functions were calculated individually for each muscle and for each subject. The resulting values were then averaged across subjects and subsequently across muscles to obtain a representative correlation value per feature. In particular, we generally expected positive correlations for temporal features, as these tend to increase with rising levels of fatigue, and negative correlation values for frequency-domain features, which typically decrease as fatigue progresses [72, 74, 75, 77]. Conversely, for spatial features, we anticipated some degree of variation, which could manifest as either positive or negative correlations depending on the specific characteristic being measured [31–33].

2.5 Statistical Analysis

To analyze the effect of fatigue without exoskeletal assistance, significant correlation values for each muscle ($p\text{-}value < 0.05$) in the WO condition were averaged and sorted. The two features with the highest absolute value of the correlation coefficient and belonging to two different domains were further analyzed. The Shapiro-Wilk test was used to assess the normality of the data (significance level set at $p\text{-}value = 0.05$). Since the results indicated a significant deviation from the normal distribution, nonparametric statistical tests were employed. In particular, differences in feature values between the W and WO conditions and across time frames were assessed using the Wilcoxon signed-rank test. Specifically, differences between the two conditions were analyzed for each monitored muscle within each fixed time frame. For each condition, pairwise comparisons of feature values between *Start*, *Middle,* and *End* frames were evaluated with Bonferroni Correction (*Start-Middle, Middle-End, Start-End, p-value = 0.0167*). Furthermore, increases in activation values

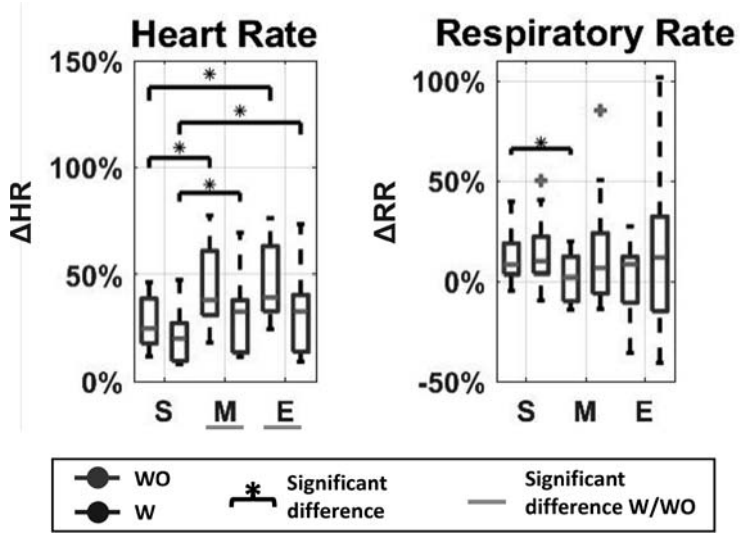

Fig. 5. Percentage increases with respect to the baseline (resting) value of HR and RR. HR showed significant increases between the *start* and the *middle*, and the *start* and *end* time frames, highlighting the insurgence of fatigue in the subjects in both conditions (W/WO). RR did not show any significant difference, except between the *start* and *middle* time frame in the WO condition.

across time frames and the two conditions were evaluated using the nonparametric two-way Scheirer-Ray-Hare test.

Moreover, to evaluate how physical effort increased among muscles, optimal linear models were fitted to each feature over time, and the resulting slopes were analyzed. Specifically, differences in slope values between conditions (W and WO) were evaluated using the Wilcoxon signed-rank test ($p\text{-}value < 0.05$).

All signal processing and statistical analyses were conducted using MATLAB software (version 2019b, MathWorks, Natick, MA, USA).

3 Results

All subjects successfully completed the full 15-minute task duration without stopping. Borg scale showed higher perceived exertion for the WO condition (WO: 15.6 ± 2.3, W: 11.1 ± 2.4, W vs. WO p-value: 9.7×10^{-4}), demonstrating the effect of the exoskeleton in reducing the perceived effort during overhead working tasks, and thus confirming our hypothesis of fatigue occurring differently in the two conditions. Average SUS scored 85.8 ± 7.0 (maximum SUS value = 100), indicating a high level of perceived usability of the exoskeleton in the performed task.

Figure 5 shows the results of the cardio-respiratory activity in the three time frames and in the W/WO conditions. The HR showed significant increases over time, with significant differences between the *Start* (S) and *Middle* (M), and between *Start* and *End* (E) time frames, indicating that the physical effort had a tangible effect on the subjects in both conditions. Significantly higher values in the WO condition compared to the W condition were found in *Middle* and *End* time frames. On the other hand, RR showed a significant decrease between *Start* and *Middle* time frames in the WO condition, but did not show any significant difference between other time frames or between the W/WO conditions.

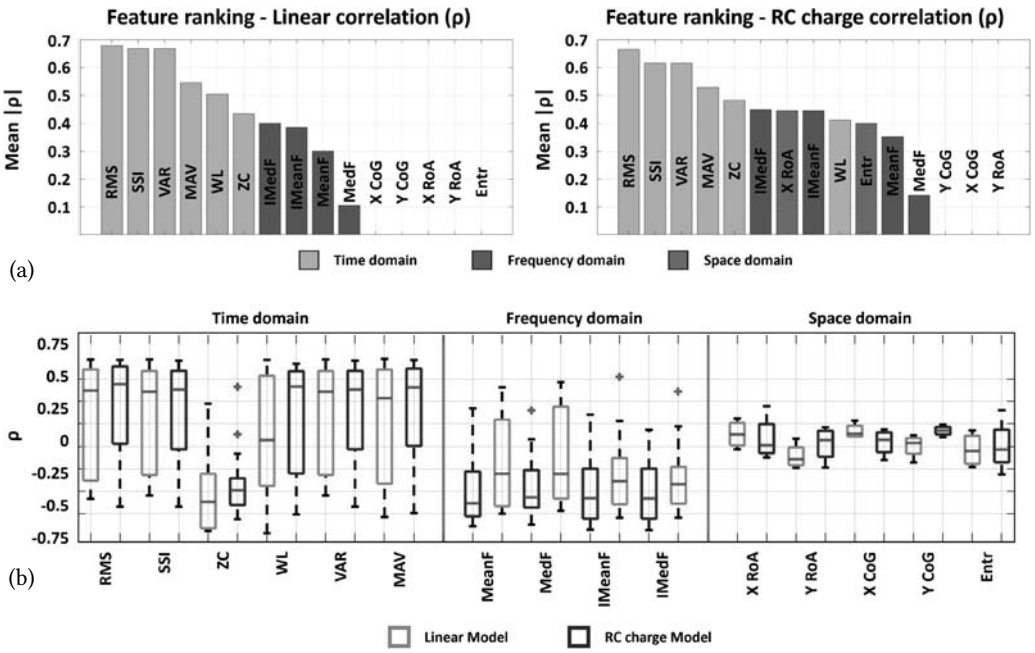

Fig. 6. Feature ranking: sorted average significant correlation absolute values (a) for the linear (left) and RC-based (right) models. With both models, RMS and IMedF achieved the highest correlation coefficients for the time and frequency domains, respectively. All correlation values for each feature for the linear (green) and RC-based (blue) models (b). All time-domain features showed positive median values, except for ZC. All frequency-domain features showed negative median values. Space-domain features showed low correlation values.

3.1 Correlation Ranking

Average and median correlation coefficients (ρ) between the features and the two workload models are presented in Figure 6: (a) shows the sorted absolute values of correlation coefficients, obtained averaging only significant correlations ($p\text{-}value \leq 0.05$); (b) shows all the obtained correlation coefficients for each feature (both significant and non-significant).

Correlation analysis showed median positive coefficients for the time-domain features, suggesting, in agreement with previous studies, that they increase with perceived physical effort over time [72]. The only exception was found for ZC, which showed a similar correlation coefficient but opposite in sign (Figure 6(b)). On the other hand, frequency-domain features showed all negative median correlation coefficients, suggesting that they decrease over time, in agreement with the literature [72]. Spatial-domain features showed the lowest correlation coefficients or no significant correlations at all, suggesting that they may not be easily associated with increasing perceived fatigue or effort.

The ranking with the linear and the RC charge models of physical effort presented similar correlation results (Figure 6(a)). In both cases, RMS (Linear $\rho RMS = 0.68$; RC $\rho RMS = 0.67$) and IMedF (Linear $\rho IMedF = 0.40$; RC $\rho IMedF = 0.45$) were identified as the most correlating features from the time and frequency domains, respectively. The two most correlating features from the time and frequency domains (RMS and IMedF) were further analyzed. The only feature that showed a different behavior compared to the others in its domain was ZC (linear $\rho ZC = 0.43$; RC $\rho ZC = 0.48$), which was therefore further analyzed. Non-significant correlations in the linear model were found

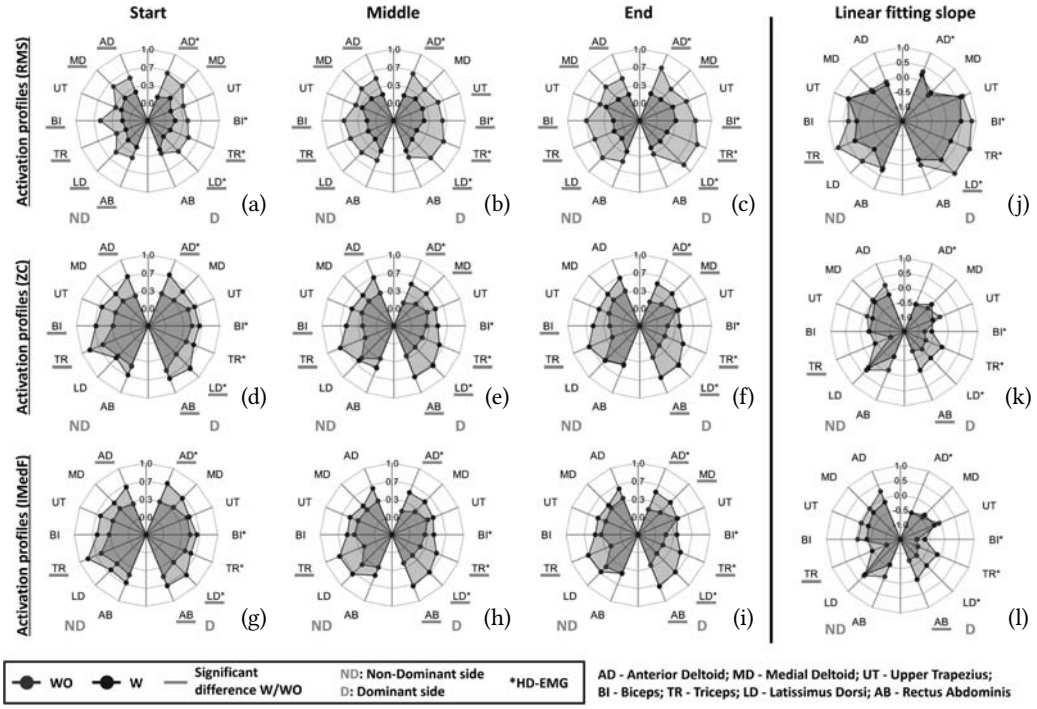

Fig. 7. RMS, ZC, and IMedF values in all the monitored muscles in W/WO conditions, in start ($0 \leq time < 5$), middle ($5 \leq time < 10$), and end ($time \geq 10$) time frames ((a)–(c), (d)–(f), (g)–(i)). Linear fitting slopes for RMS, ZC, and IMedF in each monitored muscle in W/WO conditions ((j)–(L)).

for RMS in the non-dominant AD, MD, and for the dominant AB; for ZC in the non-dominant MD and AB; for IMedF in the non-dominant MD, UT, BI, and AB, and for the dominant UT. Non-significant correlations in the RC model were found for RMS in the non-dominant AD, MD, and AB, and in the dominant AB; for ZC in the non-dominant AD, MD, and AB; for IMedF in the non-dominant AD, MD, UT, and BI.

3.2 Exoskeleton Assistance

Feature values for each muscle and W/WO condition are reported in Figure 7. Significant differences were found for both RMS and IMedF between the two conditions, with the WO condition presenting higher values of RMS and lower of IMedF for most muscles, underlying a higher instantaneous effort with respect to the W condition (Figure 7(a)–(c), (d)–(f), (g)–(1)). Interestingly, the most significant differences remained consistent across all time frames, indicating that the positive effect of the exoskeleton is tangible regardless of the subjects' perceived physical effort. RMS showed a higher number of significant differences with respect to ZC and IMedF, and higher symmetry. All significant differences identified higher values of RMS or lower values of ZC and IMedF for the W condition, suggesting that the exoskeleton assisted the users without generating any adverse effect on the muscles.

The linear regression analysis (Figure 7(j)–(l)) presented different results: while RMS slopes highlighted higher increases in the WO condition in most muscles (Figure 7(j)), ZC and IMedF showed different behaviors in the dominant and non-dominant side (Figure 7(k)–(l)). Few significant

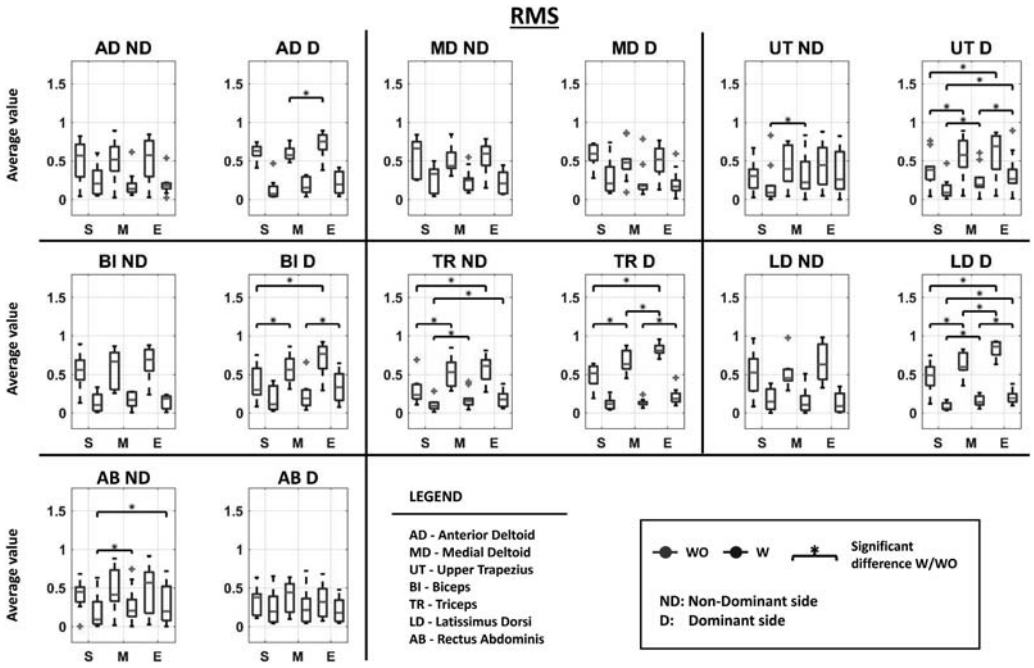

Fig. 8. RMS value in each muscle and condition (W/WO, red/blue boxes). Dominant vs. non-dominant side, for different time frames: start (S), middle (M), and end (E). Significant differences between time frames are reported.

differences were found, highlighting a higher slope of the RMS (increasing fatigue) in the non-dominant side TR, and in the dominant side LD in the WO condition, and a lower slope of the ZC and IMedF (increasing fatigue) of the non-dominant side TR, and in the dominant side AB in the WO condition.

Average feature values in the three time frames are reported in Figures 8–10. Although it is possible to see an increasing trend over time of the RMS in most muscles, the Wilcoxon pairwise analysis only identified a few significant differences, mainly in the dominant UT, BI, TR, and LD and in the non-dominant TR and AB. ZC showed significant decreasing trends in dominant AD, BI, LD, and AB and in the non-dominant TR and AB. Similarly, IMedF showed significant decreasing trends over time in the dominant AD, BI, and LD and in the non-dominant TR and AB.

The Scheirer-Ray-Hare test indicated a significant effect of exoskeleton use on RMS values across all muscles. In contrast, ZC values were significantly affected in all muscles except the dominant UT and the non-dominant ABS and LD muscles. A similar pattern was observed for IMEDF, with significant differences in all muscles except the dominant UT and non-dominant ABS. The same test revealed a significant association between RMS values and time frame in dominant UT, BI, TR, LD, and non-dominant TR. Similarly, significant correlations between ZC values and time frame were observed in dominant AD, BI and non-dominant TR. For IMEDF, significant time-related effects were found in dominant AD, BI and non-dominant TR. No significant interactions between time frame and condition were detected for any muscle or feature.

4 Discussion

This study analyzed upper body muscular activations of 10 subjects performing a 15-minute overhead task, both W and WO an exoskeleton, during an isometric contraction. From bipolar

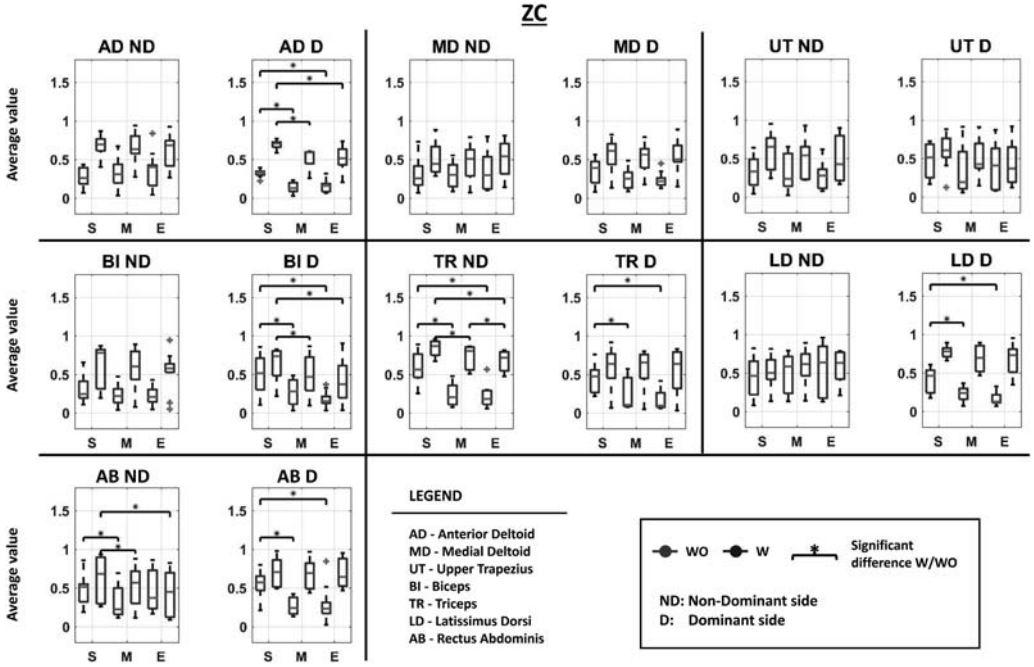

Fig. 9. ZC value in each muscle and condition (W/WO, red/blue boxes). Dominant vs. non-dominant side, for different time frames: start (S), middle (M), and end (E). Significant differences between time frames are reported.

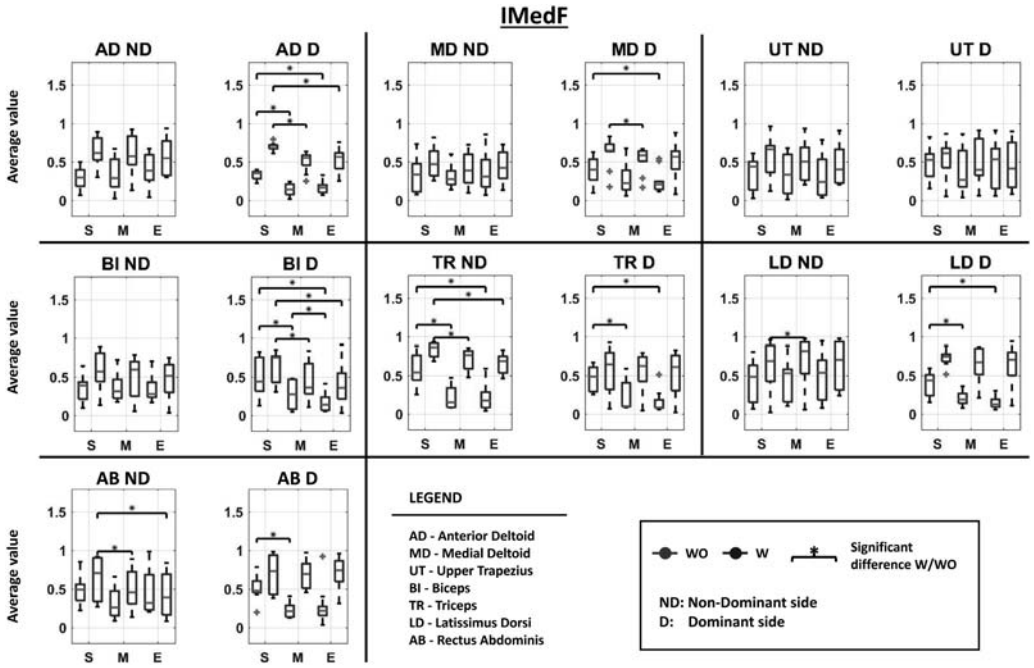

Fig. 10. IMedF value in each muscle and condition (W/WO, red/blue boxes). Dominant vs. non-dominant side, for different time frames: start (S), middle (M), and end (E). Significant differences between time frames are reported.

sEMG and HDsEMG on seven muscle pairs, commonly used temporal-, frequency-, and spatial-domain features were extracted and ranked by their correlation with overall physical effort models.

The analysis showed how commonly studied features from the time and frequency domains [72] effectively distinguished between exoskeleton-assisted and WO exoskeleton conditions for most muscles across all time frames.

Similarly to other findings in the literature, the exoskeleton demonstrated a positive impact on the supported muscles: many statistically significant differences in the activation profiles were found compared to the WO exoskeleton condition, suggesting a reduced level of fatigue [16, 18] (Figure 7). However, while most muscles exhibited significant differences in instantaneous effort between conditions (W/WO), only a few showed notable changes in the three time frames.

Results indicated that the exoskeleton-assisted condition led to reduced perceived discomfort and effort, as well as lower instantaneous effort compared to the WO exoskeleton condition. The Borg and SUS scales confirmed that subjects found the exoskeleton helpful, while HR data showed increased fatigue with higher values in the WO condition (Figure 5). However, RR did not show significant differences between conditions or over time.

Consistent with previous findings reported in the literature [72], features extracted from different signal domains exhibited distinct patterns in relation to the level of fatigue. The time-domain features demonstrated positive correlations with both proposed fatigue models, indicating an overall increase in their values as fatigue progressed. In contrast, frequency-domain features were negatively correlated, showing a general decrease in response to fatigue (Figure 6). The only exception to this trend was observed for the ZC feature, which exhibited behavior more consistent with frequency-domain features despite being typically classified as a time-domain feature. This may be due to the fact that, while computed in the time domain, ZC inherently reflects frequency-related characteristics of the signal.

While previous studies have established associations between fatigue and time-, frequency- [72], and spatial-domain features [31–33], in this study, time-domain features exhibited a higher degree of correlation with fatigue levels, suggesting their potential as more reliable indicators with sEMG data (Figure 6). Conversely, HDsEMG spatial features had lower correlations, but time- and frequency-domain features from HDsEMG still revealed significant differences between conditions, in particular with the IMedF feature (Figure 7), facilitated by the larger size of the adhesive surface of HDsEMG grids which reduced electrode positioning errors and shifts. Nonetheless, ZC and IMedF features showed higher variability in regression slope analysis, with differing behaviors on the dominant and non-dominant sides (Figure 7).

Results ranked features based on their responsiveness to fatigue and working conditions, providing useful guidelines for future research. Most features effectively identified the exoskeleton's positive impact on reducing muscular load, as supported by subjective feedback.

RMS, ZC, and IMedF showed significant differences in muscle activity with the exoskeleton, except for a few muscles, with no evidence of adverse effects.

The low correlation observed for spatial-domain features indicates their potentially limited effectiveness in low-intensity tasks. This outcome underscores the need for further investigation in high-intensity conditions, such as those explored in previous studies [27, 31–33], to better understand their utility and relevance.

Linear fitting analysis revealed minimal differences between the W and WO conditions, suggesting that despite the immediate effect of the exoskeleton on the muscular load, the increase in the physical effort was perceived in both conditions in a similar way (Figure 7).

One limitation of this study is its small, homogeneous sample of ten male participants. Given the sample size, randomization alone may not have effectively controlled for order effects or carry-over effects. Moreover, the inclusion of only male participants restricts the generalizability of the

findings. Future investigations should include a balanced representation of sexes to account for potential physiological differences in muscle activation and fatigue dynamics, increase sample size and age range, and explore the effects of features in shorter, more intense tasks. Furthermore, the results of this study should be interpreted in the context of the specific overhead task that was performed. The findings are task-dependent and may not generalize to other types of physical activity or postural demands, as the aim of this work was to evaluate the behavior of different feature domains in the context of a defined, controlled working scenario. Given the specificity of the task and the features assessed, additional studies will be necessary to explore the generalizability of these findings to other tasks, postures, or operational settings. Additionally, studying these features with real workers in actual working conditions could provide more accurate and applicable insights.

Nonetheless, the results of this study demonstrated the potential for effectively monitoring worker fatigue levels within an Industry 5.0 scenario.

5 Conclusions

This study presented a systematic feature selection strategy based on correlations with overall fatigue patterns, identifying key EMG characteristics closely associated with perceived physical exertion. The proposed approach was tested in an occupationally relevant scenario by recruiting 10 healthy participants, who were asked to perform a prolonged fatiguing task involving isometric contractions. This setting allowed us to investigate the responsiveness of different sEMG features to physical effort and fatigue under realistic working conditions.

The application of the proposed approach enabled the identification of EMG metrics that consistently highlighted physical fatigue across two different fatigue models: a linear model and a representation-based model derived from RC charge dynamics. Results demonstrated that time-domain features were more effective than frequency- and space-domain features in detecting fatigue during prolonged, low-intensity isometric tasks.

The identified metrics were then used to compare the level of physical fatigue between two conditions: a condition WO exoskeleton task execution and while wearing an occupational exoskeleton. Analysis with the selected EMG metrics showed their effectiveness in highlighting the reduced load on the monitored muscles gained from the exoskeleton use.

In general, the findings of this study contribute to strengthening the methodological foundations for using EMG metrics to monitor physical fatigue during sustained isometric activities. Future work will aim to extend this analysis to dynamic occupational tasks, moving beyond static isometric exercises to capture muscle activity in more realistic, operational scenarios.

References

[1] Ambra Giustetto, Fabio Vieira Dos Anjos, Francesca Gallo, Rossella Monferino, Giacinto Luigi Cerone, Massimo Di Pardo, Marco Gazzoni, and Margherita Micheletti Cremasco. 2021. Investigating the effect of a passive trunk exoskeleton on local discomfort, perceived effort and spatial distribution of back muscles activity. *Ergonomics* 64, 11 (2021), 1379–1392.

[2] J. de Kok, P. Vroonhof, J. Snijders, G. Roullis, M. Clarke, K. Peereboom, P. van Dorst, and I. Isusi. 2019. Work-Related Musculoskeletal Disorders: Prevalence, Costs and Demographics in the EU. European Agency for Safety and Health at Work. Retrieved from https://osha.europa.eu/sites/default/files/Work_related_MSDs_prevalence_costs_and_demographics_in_EU_summary

[3] Karsten Dreinhöfer and Natalie Watfa Watfa. 2022. The burden. In *The EFORT White Book "Orthopaedics and Traumatology in Europe."* J.A.N. Verhaar, P. Kjærsgaard-Andersen, D. Limb, K-P Günther, and Th. Karachalios (Eds.), Dennis Barber Ltd., 11–27. DOI: 10.1922/EFORTWhitebook2022

[4] Institute for Health Metrics and Evaluation. 2020. GBD Results. Institute for Health Metrics and Evaluation, University of Washington. Retrieved September 1, 2021 from http://ghdx.healthdata.org/gbd-results-tool

[5] R. Anagha and A. S. Xavier. 2020. A review on ergonomic risk factors causing musculoskeletal disorders among construction workers. *International Journal of Engineering Research and Technology* 9, 07 (2020), 1234–1236.

[6] Stephen Bao, Ninica Howard, and Jia-Hua Lin. 2019. Are work-related musculoskeletal disorders claims related to risk factors in workplaces of the manufacturing industry? *Annals of Work Exposures and Health* 64, 11 (2019), 152–164.
[7] Peter W. Buckle and J. Jason Devereux. 2002. The nature of work-related neck and upper limb musculoskeletal disorders. *Applied Ergonomics* 33, 3 (2002), 207–217.
[8] Y. Roquelaure. 2018. Musculoskeletal disorders and psychosocial factors at work. *ETUI Research Paper* 142 (2018), 82.
[9] Christian Tamantini, Fabrizio Marra, Joshua Di Tocco, Stefano Di Modica, Antonio Lanata, Francesca Cordella, Maurizio Ferrarin, Francesco Rizzo, Mara Stefanelli, Maddalena Papacchini, et al. 2025. Senserisc: An instrumented smart shirt for risk prevention in the workplace. *Wearable Technologies* 6 (2025), e20.
[10] Alberto Ranavolo, Francesco Draicchio, Tiwana Varrecchia, Alessio Silvetti, and Sergio Iavicoli. 2018. Erratum: Alberto, r. et al., wearable monitoring devices for biomechanical risk assessment at work: Current status and future challenges—a systematic review. int. j. environ. res. public health 2018, 15, 2001. *International Journal of Environmental Research and Public Health* 15 (Nov. 2018), 2569.
[11] Alberto Ranavolo, Arash Ajoudani, Andrea Cherubini, Matteo Bianchi, Lars Fritzsche, Sergio Iavicoli, Massimo Sartori, Alessio Silvetti, Bram Vanderborght, Tiwana Varrecchia, et al. 2020. The sensor-based biomechanical risk assessment at the base of the need for revising of standards for human ergonomics. *Sensors* 20 (Oct. 2020), 1–15.
[12] Theocharis Chatzis, Dimitrios Konstantinidis, and Kosmas Dimitropoulos. 2022. Automatic ergonomic risk assessment using a variational deep network architecture. *Sensors* 22, 16 (2022), 6051.
[13] Beatrice Albanesi, Michela Piredda, Marco Bravi, Federica Bressi, Raffaella Gualandi, Anna Marchetti, Gabriella Facchinetti, Andrea Ianni, Francesca Cordella, Loredana Zollo, et al. 2022. Interventions to prevent and reduce work-related musculoskeletal injuries and pain among healthcare professionals. A comprehensive systematic review of the literature. *Journal of Safety Research* 82 (2022), 124–143.
[14] F. V. dos Anjos, M. Ghislieri, G. L. Cerone, T. P. Pinto, and M. Gazzoni. 2022. Changes in the distribution of muscle activity when using a passive trunk exoskeleton depend on the type of working task: A high-density surface EMG study. *Journal of Biomechanics* 130 (2022), 110846.
[15] Jean Theurel and Kevin Desbrosses. 2019. Occupational exoskeletons: Overview of their benefits and limitations in preventing work-related musculoskeletal disorders. *IISE Transactions on Occupational Ergonomics and Human Factors* 7, 3–4 (2019), 264–280.
[16] Michiel P. de Looze, Tim Bosch, Frank Krause, Konrad S. Stadler, and Leonard W. O'Sullivan. 2016. Exoskeletons for industrial application and their potential effects on physical work load. *Ergonomics* 59, 5 (2016), 671–681.
[17] Maury A. Nussbaum, Brian D. Lowe, Michiel de Looze, Carisa Harris-Adamson, and Marty Smets. 2019. An introduction to the special issue on occupational exoskeletons. In *IISE Transactions on Occupational Ergonomics and Human Factors* 7 (3–4), 153–62. DOI:10.1080/24725838.2019.1709695
[18] Arthur van der Have, Marco Rossini, Carlos Rodriguez-Guerrero, Sam Van Rossom, and Ilse Jonkers. 2022. The exo4work shoulder exoskeleton effectively reduces muscle and joint loading during simulated occupational tasks above shoulder height. *Applied Ergonomics* 103 (2022), 103800.
[19] Simona Crea, Philipp Beckerle, Michiel De Looze, Kevin De Pauw, Lorenzo Grazi, Tjaša Kermavnar, Jawad Masood, Leonard W. O'Sullivan, Ilaria Pacifico, Carlos Rodriguez-Guerrero, et al. 2021. Occupational exoskeletons: A roadmap toward large-scale adoption. methodology and challenges of bringing exoskeletons to workplaces. *Wearable Technologies* 2 (2021), e11.
[20] Shirley A. Elprama, Jorre T. A. Vannieuwenhuyze, Sander De Bock, Bram Vanderborght, Kevin De Pauw, Romain Meeusen, and An Jacobs. 2020. Social processes: What determines industrial workers' intention to use exoskeletons? *Human Factors* 62, 3 (2020), 337–350. PMID: 31971838.
[21] Shirley A. Elprama, Bram Vanderborght, and An Jacobs. 2022. An industrial exoskeleton user acceptance framework based on a literature review of empirical studies. *Applied Ergonomics* 100 (2022), 103615.
[22] Sander De Bock, Jo Ghillebert, Renée Govaerts, Bruno Tassignon, Carlos Rodriguez-Guerrero, Simona Crea, Jan Veneman, Joost Geeroms, Romain Meeusen, and Kevin De Pauw. 2022. Benchmarking occupational exoskeletons: An evidence mapping systematic review. *Applied Ergonomics* 98 (2022), 103582.
[23] Alberto Ranavolo, Tiwana Varrecchia, Sergio Iavicoli, Agnese Marchesi, Martina Rinaldi, Mariano Serrao, Silvia Conforto, Mario Cesarelli, and Francesco Draicchio. 2018. Surface electromyography for risk assessment in work activities designed using the "revised niosh lifting equation". *International Journal of Industrial Ergonomics* 68 (Nov. 2018), 34–45.
[24] Tim Bosch, Jennifer van Eck, Karlijn Knitel, and Michiel de Looze. 2016. The effects of a passive exoskeleton on muscle activity, discomfort and endurance time in forward bending work. *Applied Ergonomics* 54 (2016), 212–217.
[25] Michail Arvanitidis, Nikolaos Bikinis, Stylianos Petrakis, Afroditi Gkioka, Dimitrios Tsimpolis, Deborah Falla, and Eduardo Martinez-Valdes. 2021. Spatial distribution of lumbar erector spinae muscle activity in individuals with and without chronic low back pain during a dynamic isokinetic fatiguing task. *Clinical Biomechanics (Bristol, Avon)* 81 (2021), 105214.

[26] Deborah Falla and Alessio Gallina. 2020. New insights into pain-related changes in muscle activation revealed by high-density surface electromyography. *Journal of Electromyography and Kinesiology: Official Journal of the International Society of Electrophysiological Kinesiology* 52 (2020), 102422.

[27] Tiwana Varrecchia, Alberto Ranavolo, Giorgia Chini, Alessandro De Nunzio, Francesco Draicchio, Eduardo Martinez-Valdes, Deborah Falla, and Silvia Conforto. High-density surface electromyography allows to identify risk conditions and people with and without low back pain during fatiguing frequency-dependent lifting activities. *Journal of Electromyography and Kinesiology: Official Journal of the International Society of Electrophysiological Kinesiology* 73 (2023), 102839–102811.

[28] Afshin Samani, Andreas Holtermann, Karen Søgaard, and Pascal Madeleine. 2010. Active biofeedback changes the spatial distribution of upper trapezius muscle activity during computer work. *European Journal of Applied Physiology* 110, 2 (2010), 415–423.

[29] Dario Farina and Aleš Holobar. 2016. Characterization of human motor units from surface EMG decomposition. *Proceedings of the IEEE* 104, 2 (2016), 353–373.

[30] Francesco Negro, Silvia Muceli, Anna Margherita Castronovo, Ales Holobar, and Dario Farina. 2016. Multi-channel intramuscular and surface EMG decomposition by convolutive blind source separation. *Journal of Neural Engineering* 13, 2 (Feb. 2016), 026027.

[31] Tiwana Varrecchia, Alberto Ranavolo, Silvia Conforto, Alessandro De Nunzio, Michail Arvanitidis, Francesco Draicchio, and Deborah Falla. 2021. Bipolar versus high-density surface electromyography for evaluating risk in fatiguing frequency-dependent lifting activities. *Applied Ergonomics* 95 (Sep. 2021), 103456.

[32] Andy Sanderson, Eduardo Martinez-Valdes, Nicola R. Heneghan, Carlos Murillo, Alison Rushton, and Deborah Falla. 2019. Variation in the spatial distribution of erector spinae activity during a lumbar endurance task in people with low back Pain. *Journal of Anatomy* 234 (2019), 532–542. DOI: https://doi.org/10.1111/joa.12935

[33] Eduardo Martinez-Valdes, Fiona Wilson, Neil Fleming, Sarah Jane McDonnell, Alex Horgan, and Deborah Falla. 2019. Rowers with a recent history of low back pain engage different regions of the lumbar erector spinae during rowing. *Journal of Science and Medicine in Sport* 22, 07 (2019), 1206–1212.

[34] Deborah Falla and Paul W. Hodges. 2017. Individualized exercise interventions for spinal pa. *Exercise and Sport Sciences Reviews* 45, 2 (2017), 105–115.

[35] Mark Robinson, Lei Lu, Ying Tan, Denny Oetomo, and Chris Manzie. 2022. Feature identification framework for back injury risk in repetitive work with application in sheep shearing. *IEEE Transactions on Bio-Medical Engineering* 70, 2 (Aug. 2022), 616–627.

[36] Jean Theurel, Kevin Desbrosses, Terence Roux, and Adriana Savescu. 2018. Physiological consequences of using an upper limb exoskeleton during manual handling tasks. *Applied Ergonomics* 67 (Feb. 2018), 211–217.

[37] Junqing Meng, Bi Zhao, Yechao Ma, Yiyu Ji, and Baisheng Nie. 2014. Effects of fatigue on the physiological parameters of labor employees. *Natural Hazards* 74 (Nov. 2014), 1127–1140.

[38] Wei Wei, Wei Wang, Zhicheng Qu, Jihua Gu, Xichuan Lin, and Chunfeng Yue. 2020. The effects of a passive exoskeleton on muscle activity and metabolic cost of energy. *Advanced Robotics* 34, 1 (2020), 19–27.

[39] Mohammad Mehdi Alemi, Saman Madinei, Sunwook Kim, Divya Srinivasan, and Maury A. Nussbaum. 2020. Effects of two passive back-support exoskeletons on muscle activity, energy expenditure, and subjective assessments during repetitive lifting. *Human Factors* 62, 3 (2020), 458–474.

[40] Christian Tamantini, Francesca Cordella, Nevio Luigi Tagliamonte, Ilenia Pecoraro, Iolanda Pisotta, Alessandra Bigioni, Federica Tamburella, Matteo Lorusso, Marco Molinari, and Loredana Zollo. 2024. A data-driven fuzzy logic method for psychophysiological assessment: An application to exoskeleton-assisted walking. *IEEE Transactions on Medical Robotics and Bionics* 6, 2 (2024), 695–705.

[41] Jong-Won Lee and Gyoosuk Kim. 2019. Design and control of a lifting assist device for preventing lower back injuries in industrial athletes. *International Journal of Precision Engineering and Manufacturing* 20 (Jun. 2019), 1825–1838.

[42] Hanjun Park, Sunwook Kim, Maury Nussbaum, and Divya Srinivasan. 2021. Effects of using a whole-body powered exoskeleton during simulated occupational load-handling tasks: A pilot study. *Applied Ergonomics* 98 (Sep. 2021), 103589.

[43] Sofía Iranzo, Alicia Piedrabuena, Daniel Iordanov, Ursula Martinez-Iranzo, and Juan Manuel Belda Lois. 2020. Ergonomics assessment of passive upper-limb exoskeletons in an automotive assembly plant. *Applied Ergonomics* 87 (Sep. 2020), 103120.

[44] Lorenzo Grazi, Emilio Trigili, Giulio Proface, Francesco Giovacchini, Simona Crea, and Nicola Vitiello. 2020. Design and experimental evaluation of a semi-passive upper-limb exoskeleton for workers with motorized tuning of assistance. *IEEE Transactions on Neural Systems and Rehabilitation Engineering* 28, 10 (Aug. 2020), 2276–2285.

[45] Frédérique Dupuis, Gisela Sole, Craig Wassinger, Mathieu Bielmann, Laurent J. Bouyer, and Jean-Sébastien Roy. 2021. Fatigue, induced via repetitive upper-limb motor tasks, influences trunk and shoulder kinematics during an upper limb reaching task in a virtual reality environment. *PloS One* 16, 4 (2021), e0249403.

[46] D. David Ebaugh, Philip W. McClure, and Andrew R. Karduna. 2006. Effects of shoulder muscle fatigue caused by repetitive overhead activities on scapulothoracic and glenohumeral kinematics. *Journal of Electromyography and Kinesiology: Official Journal of the International Society of Electrophysiological Kinesiology* 16, 3 (2006), 224–235.

[47] Hayder A. Yousif, Ammar Zakaria, Norasmadi Abdul Rahim, Ahmad Faizal Bin Salleh, Mustafa Mahmood, Khudhur A. Alfarhan, Latifah Munirah Kamarudin, Syed Muhammad Mamduh, Ali Majid Hasan, and Moaid K. Hussain. 2019. Assessment of muscles fatigue based on surface EMG signals using machine learning and statistical approaches: A review. In *IOP Conference Series: Materials Science and Engineering*, Vol. 705, IOP Publishing, 012010.

[48] G. Venugopal, M. Navaneethakrishna, and S. Ramakrishnan. 2014. Extraction and analysis of multiple time window features associated with muscle fatigue conditions using SEMG signals. *Expert Systems with Applications* 41, 6 (2014), 2652–2659.

[49] Fauzani N. Jamaluddin, Siti A. Ahmad, Samsul Bahari Mohd Noor, Wan Zuha Wan Hassan, and Y. Azhar. 2017. Features selection for Bayes classification of prolonged fatigue on rectus femoris muscle. In *2017 39th Annual International Conference of the IEEE Engineering in Medicine and Biology Society (EMBC),* Vol. 2017, IEEE, 2506-2509. DOI: 10.1109/EMBC.2017.8037366

[50] Nurul Fauzani Jamaluddin, Fatimah Ibrahim, and Siti Ahmad. 2023. A new approach to noninvasive-prolonged fatigue identification based on surface EMG time-frequency and wavelet features. *Journal of Healthcare Engineering* 2023 (Jan. 2023), 1–15.

[51] Emma J. Ratke, Hannah McMaster, Chris L. Vellucci, Dennis J. Larson, Michael W. R. Holmes, and Shawn M. Beaudette. 2025. Ability of a passive back support exoskeleton to mitigate fatigue related adaptations in a complex repetitive lifting task. *Journal of Biomechanics* 181 (2025), 112553.

[52] Mislav Jordanić, Mónica Rojas-Martínez, Miguel Angel Mañanas, Joan Francesc Alonso, and Hamid Reza Marateb. 2017. A novel spatial feature for the identification of motor tasks using high-density electromyography. *Sensors* 17, 7 (2017), 1597.

[53] P. A. Karthick, Diptasree Maitra Ghosh, and S. Ramakrishnan. 2018. Surface electromyography based muscle fatigue detection using high-resolution time-frequency methods and machine learning algorithms. *Computer Methods and Programs in Biomedicine* 154 (2018), 45–56.

[54] Abdulhamit Subasi and M. Kemal Kiymik. 2010. Muscle fatigue detection in EMG using time–frequency methods, ICA and neural networks. *Journal of Medical Systems* 34 (2010), 777–785.

[55] Laura A. Frey-Law, John M. Looft, and Jesse Heitsman. 2012. A three-compartment muscle fatigue model accurately predicts joint-specific maximum endurance times for sustained isometric tasks. *Journal of Biomechanics* 45, 10 (2012), 1803–1808.

[56] Maxime Yochum, Stéphane Binczak, Toufik Bakir, S. Jacquir, and R. Lepers. 2010. A mixed fes/emg system for real time analysis of muscular fatigue. In *2010 Annual International Conference of the IEEE Engineering in Medicine and Biology*. IEEE, 4882–4885.

[57] Nikhil V. Divekar, Gray C. Thomas, Avani R. Yerva, Hannah B. Frame, and Robert D. Gregg. 2024. A versatile knee exoskeleton mitigates quadriceps fatigue in lifting, lowering, and carrying tasks. *Science Robotics* 9, 94 (2024), eadr8282.

[58] Pranav Madhav Kuber, Hrushikesh Godbole, and Ehsan Rashedi. 2024. Detecting fatigue during exoskeleton-assisted trunk flexion tasks: A machine learning approach. *Applied Sciences* 14, 9 (2024), 3563.

[59] Pranav Madhav Kuber, Abhineet Rajendra Kulkarni, and Ehsan Rashedi. 2024. How effective are forecasting models in predicting effects of exoskeletons on fatigue progression? *Sensors* 24, 18 (2024), 5971.

[60] Lukas Bergmann, Lea Hansmann, Philip von Platen, Steffen Leonhardt, and Chuong Ngo. 2024. Fatigue assessment and control with lower limb exoskeletons. *IEEE Transactions on Human-Machine Systems* 55 (2024), 10–22.

[61] Haizhe Jin, Meng Xiao, Li Liu, Shuang Kan, Yongyan Fu, and Dawei Zhang. 2024. Relationship between physical fatigue and mental fatigue based on multimodal measurement under different load levels. *Ergonomics* 67, 11 (2024), 1748–1763.

[62] Garrick N. Forman, Sophia A. Nikitin, Cameron J. Lang, David A. Gabriel, Michael W. Sonne, Aaron M. Kociolek, and Michael W. R. Holmes. 2025. Impact of repetitive mouse aiming on muscle fatigue and fine motor performance of the distal upper limb. *Journal of Electromyography and Kinesiology: Official Journal of the International Society of Electrophysiological Kinesiology* 82 (2025), 102992.

[63] Giorgia Coraggio, Mattia Cera, Marco Cirelli, and Pier Paolo Valentini. 2024. Review and comparison of linear algorithms to quantify muscle fatigue based on SEMG signals. *Ergonomics* 67, 11 (2024), 1729–1747.

[64] Luka Peternel, Nikos Tsagarakis, Darwin Caldwell, and Arash Ajoudani. 2018. Robot adaptation to human physical fatigue in human–robot co-manipulation. *Autonomous Robots* 42 (Jun. 2018), 1–11.

[65] Hermie J. Hermens, Bart Freriks, Catherine Disselhorst-Klug, and Günter Rau. 2000. Development of recommendations for SEMG sensors and sensor placement procedures. *Journal of Electromyography and Kinesiology: Official Journal of the International Society of Electrophysiological Kinesiology* 10, 5 (2000), 361–374.

[66] Giulia Ramella, Lorenzo Grazi, Francesco Giovacchini, Emilio Trigili, Nicola Vitiello, and Simona Crea. 2024. Evaluation of antigravitational support levels provided by a passive upper-limb occupational exoskeleton in repetitive arm movements. *Applied Ergonomics* 117 (2024), 104226.
[67] Sandra K. Hunter. 2014. Sex differences in human fatigability: Mechanisms and insight to physiological responses. *Acta Physiologica* 210, 4 (2014), 768–789.
[68] Matthew S. Tenan, Anthony C. Hackney, and Lisa Griffin. 2016. Maximal force and tremor changes across the menstrual cycle. *European Journal of Applied Physiology* 116, 1 (2016), 153–160.
[69] Gunnar A. Borg. 1982. Psychophysical bases of perceived exertion. *Medicine and Science in Sports and Exercise* 14, 5 (1982), 377–384.
[70] Aaron Bangor, Phil Kortum, and James Miller. 2009. Determining what individual sus scores mean: Adding an adjective rating scale. *Journal of Usability Studies* 4 (Apr. 2009), 114–123.
[71] Christian Tamantini, Francesco Scotto di Luzio, Claudiu Hromei, Lorenzo Cristofori, Danilo Croce, Marco Cammisa, Arcangela Cristofaro, Maria Vittoria Marabello, Roberto Basili, and Loredana Zollo. 2023. Integrating physical and cognitive interaction capabilities in a robot-aided rehabilitation platform. *IEEE Systems Journal* 17, 4 (Jan. 2023), 1–12.
[72] Jiaqi Sun, Guangda Liu, Yubing Sun, Kai Lin, Zijian Zhou, and Jing Cai. 2022. Application of surface electromyography in exercise fatigue: A review. *Frontiers in Systems Neuroscience* 16 (2022), 893275. DOI: 10.3389/fnsys.2022.893275
[73] Dick F. Stegeman, Bert U. Kleine, Bernd G. Lapatki, and Johannes P. Van Dijk. 2012. High-density surface EMG: Techniques and applications at a motor unit level. *Biocybernetics and Biomedical Engineering* 32, 3 (2012), 3–27.
[74] R. Merletti, B. Afsharipour, J. Dideriksen, and D. Farina. 2016. Muscle force and myoelectric manifestations of muscle fatigue in voluntary and electrically elicited contractions. In *Surface Electromyography: Physiology, Engineering, and Applications*, Roberto Merletti and Dario Farina (Eds.), Wiley, 273–310. DOI: 10.1002/9781119082934.ch10
[75] Roberto F. Pitzalis, Beatrice Lagomarsino, Indya Ceroni, Nicholas Cartocci, Jamil Ahmad, Giulia A. Albanese, Jacopo Zenzeri, Christian Di Natali, Darwin G. Caldwell, Maura Casadio, et al. 2025. Evaluating muscle fatigue with non-invasive approaches: A review of methods, metrics and implications. *IEEE Transactions on Neural Systems and Rehabilitation Engineering* 33 (2025), 1–1.
[76] Stephen R. Alty and Apostolos Georgakis. 2011. Mean frequency estimation of surface EMG signals using filterbank methods. In *2011 19th European Signal Processing Conference*. IEEE, 1387–1390.
[77] Madeleine M. Lowery and Mark J. O'Malley. 2003. Analysis and simulation of changes in EMG amplitude during high-level fatiguing contractions. *IEEE Transactions on Bio-Medical Engineering* 50, 9 (2003), 1052–1062.

Received 25 November 2024; revised 27 July 2025; accepted 31 July 2025